Indonesian Journal of Electrical Engineering and Computer Science
Vol. 43, No. 2, August 2026, pp. 363~383
ISSN: 2502-4752, DOI: 10.11591/ijeecs.v43.i2.pp363-383

Improved sizing of a damped passive filter for harmonic attenuation using a teaching-learning-based optimization algorithm for an industrial site

Brahimi Omar, Rabah Djekidel, Hadjadj Abdechafik, Sid Ahmed Bessedik
LACoSERE laboratory, Department of Electrical Engineering, Faculty of Technology, Ammar Telidji University of Laghouat, Laghouat, Algeria

Article Info

Article history:

Received Mar 10, 2026
Revised Jun 16, 2026
Accepted Jun 27, 2026

Keywords:

Damped passive filter
Harmonics
Non-linear load
Power quality analyzer Fluke 438-II
TLBO

ABSTRACT)

Based on measurements of current harmonics that adversely affect power quality in an industrial setting, and to ensure compliance with permissible levels according to IEEE 519, this paper aims to compare the effectiveness of conventional and optimized sizing of damped passive filter components to reduce total harmonic distortion (THD) and improve the power factor (PF). The optimization of passive filter element values relies on a powerful metaheuristic algorithm called teaching-learning-based optimization (TLBO). Simulation results show that the THD of current and voltage reach values of 17.34% and 8.61%, respectively, and decrease to very low values after implementation of the damped passive filter in the optimal case using the TLBO algorithm. The results also demonstrated a proportional relationship between the harmonic currents in the load and the overall increase in losses in the transformer. Optimizing the damped passive filter reduced harmonic distortion, improved the PF, and limited energy losses, thus confirming the superior ability of this algorithm to identify a very high-efficiency solution.

Corresponding Author:

Rabah Djekidel
LACoSERE laboratory, Department of Electrical Engineering, Faculty of Technology
Université Amar Telidji 37G Route de Ghardaia
Laghouat, 03000, Algeria
Email: r.djekidel@lagh-univ.dz

1. INTRODUCTION

Electricity distributors seek to provide high-quality electrical energy to customers in accordance with applicable standards. However, electrical energy is subject to numerous disturbances during transmission and distribution before reaching end users [1], [2]. These disturbances are generally related to the physical and operational characteristics of electrical network equipment [3], [4]. Among them, harmonics are considered one of the most significant power quality problems caused by the increasing use of non-linear electrical loads [5]–[7]. Such loads distort current waveforms, producing undesirable effects including overheating, malfunction, premature ageing of machinery and cables, and reduced network efficiency [8]–[10].

Transformers are particularly sensitive to harmonic distortion. Harmonics increase iron-core losses, including eddy-current and hysteresis losses, and may cause abnormal winding temperatures, thereby reducing transformer efficiency and service life. The IEEE C57.110 standard provides guidance for transformer operation under non-sinusoidal current conditions and highlights the potential derating of transformer capacity caused by harmonics [11].

Generally, to address the problem of harmonics in electrical installations, avoid their negative repercussions, improve the power factor (PF), and reduce reactive power transmission, thus avoiding losses and costs, and ensure the quality of electrical energy, numerous harmonic control methods are often used, including those based on the use of filtering devices such as passive, active, and hybrid filters [8]–[10]. Passive filters, based on (RLC) components tuned to specific harmonic frequencies, are widely used because they can simultaneously attenuate harmonics and compensate reactive power, thereby reducing losses and voltage drops. Nevertheless, passive filters may suffer from resonance problems and limited compensation capability [12]–[14]. Active filters constitute an alternative solution by generating compensating harmonic currents to cancel network harmonics [15], [16], while hybrid filters combine passive and active techniques to achieve a compromise between performance and cost [17]. Conventional passive filter sizing is generally based on a simple sequential calculation using the load harmonic spectrum and source impedance [18]–[24]. Although this method can provide acceptable results [25]–[28], it remains approximate and cannot guarantee optimal performance owing to network impedance variations and harmonic interactions. Continuous theoretical and experimental investigations have improved the understanding of harmonic behaviour and filtering techniques [29]–[31], contributing to the development of standards such as IEEE 519 and EN 50160, which define acceptable harmonic distortion limits in electrical networks [32]–[36].

More recently, meta-heuristic optimization algorithms inspired by biological and social behaviours, including genetic algorithms (GA), particle swarm optimization (PSO), and teaching-learning-based optimization (TLBO), have been introduced to enhance harmonic filtering and power quality performance [37]–[40]. Despite these advances, studies addressing harmonic mitigation through optimized passive and active filtering strategies using meta-heuristic algorithms remain relatively limited [41]–[47].

Previous studies on passive filter optimization, based on single-objective or multi-objective approaches, have primarily focused on electrical criteria such as THD, resonant impedance, reactive power, or cost, without incorporating transformer losses, which are nevertheless crucial for energy efficiency and thermal behavior. These limitations motivate our contribution, which is based on a passive filtering optimization strategy aimed at simultaneously reducing harmonic distortion and improving the PF without exacerbating resonance phenomena. The novelty of this study lies in the combination of an objective analytical function, derived from the physical relationship of the PF in the presence of harmonics, which simultaneously reduces overall harmonic distortion and corrects the PF; in addition to integrating the analysis of the various losses in the electrical transformer, allowing for a more consistent optimization that accurately reflects the system’s actual energy performance.

The objective of this study is to perform a comparative analysis, using numerical simulation, of a conventional and an optimal design for a second-order parallel high-pass passive filter, based on the TLBO optimization algorithm due to its excellent characteristics of flexibility, robustness, and ease of implementation [46]–[48]. This analysis evaluates the filter’s effectiveness in mitigating harmonics generated by a polluted load and compensating reactive power, while quantifying harmonic-induced iron and copper losses in the distribution transformer using the IEEE C57.110 calculation method to ensure accurate loss assessment under harmonic conditions. Measurements were conducted at an industrial maintenance site in the Laghouat region of south-central Algeria using a Fluke 438-II power quality analyser.

2. METHOD

The proposed methodology combines the study of harmonic disturbances and their effects on electrical transformers, the analysis of harmonic filtering techniques, the modeling of an electrical circuit polluted by nonlinear loads, and the application of an optimization technique to determine the optimal parameters of the filter and improve the quality of the power.

2.1. Harmonic disturbance and its effect on electrical transformer

Power grids are mainly impacted by waveform distortions due to the presence of nonlinear loads based on power electronics components, since the current they consume often deviates from the pure sinusoidal shape [49], [50]. This means that voltage distortion is inevitable once current distortion occurs [51]–[53]. The harmonic signal can be decomposed into a collection of sinusoidal signals, each of which has two components: a sinusoidal signal with the fundamental frequency, and sinusoidal signals with a multiple frequency of that of the fundamental component, which is the harmonic quantity. The usable harmonic filters are classified into three main types depending on the harmonic source application: passive filter, active filter and hybrid filter [50]–[53]. The presence of a signal containing harmonic disturbances is generally confirmed using an indicator called total harmonic distortion (THD) and by consuming the distorting power by non-linear loads. There are two types of THD: voltage THD (at the source) and current THD (due to the loads). For the harmonic current; the THD is calculated as follows [50]–[53]:

$$THD_i = \frac{\sqrt{\sum_{h=2}^{h=n} I_h^2}}{I_1} \quad (1)$$

where, I_h is the value of the current harmonics; I_1 is the value of the fundamental current component; h is the harmonic order considered; n is the maximum rank of the harmonics considered. For the voltage, the THD is expressed by [50]–[53]:

$$THD_v = \frac{\sqrt{\sum_{h=2}^{h=n} V_h^2}}{V_1} \quad (2)$$

where, V_h is the harmonic component of voltage; V_1 is the voltage of the fundamental component.

The PF is an indicator of the quality and efficiency of an electrical system; it is related to reactive power consumption. In the presence of current and voltage harmonics, the PF decreases, and active and reactive power are expressed as follows [50]–[53].

$$P_l = \sum_{h=1}^{h=n} V_h I_h \cos \phi_h \quad (3)$$

$$Q_l = \sum_{h=1}^{h=n} V_h I_h \sin \phi_h \quad (4)$$

The distortion power D_l that makes it possible to take into account harmonics can be calculated by the following relation [50]–[53]:

$$D_l = V_1 \sqrt{\sum_{h=2}^{h=n} I_h^2} \quad (5)$$

the PF is directly linked by the ratio between the active power P_l and the apparent power S_l; it is expressed by the relationship below [50]–[53]:

$$PF = \frac{P_l}{S_l} = \frac{P_l}{\sqrt{P_l^2 + {Q_l}^2 + {D_l}^2}} = PF_{dis} \times \cos(\varphi_1) \quad (6)$$

where, PF_{dis} expresses the distortion factor; φ_1 represents the phase shift between the fundamental current and the voltage.

Due to reactive power, which can cause energy losses and PF degradation, the latter can be improved to compensate for this reactive power by integrating capacitors into the electrical installation [52]–[56]:

$$Q_c = Q_l - Q_l^{'} = P_l(tg\varphi_1 - tg\varphi_2) \quad (7)$$

where, Q_c is the reactive power that must be compensated.

The fundamental effect of harmonics on transformers is an increase in losses and, consequently, machine heating. This effect manifests itself both as Joule losses and as additional losses, which can be classified as load losses and no-load losses [57]–[59]. The IEEE C57.110 standard provides methods for determining the additional heating of electrical equipment under the influence of harmonics [60]. No-load losses are caused by hysteresis and eddy currents. Load losses due to harmonics are divided into two categories: Joule losses in the copper of the transformer windings and additional losses due to eddy currents, it can be determined by short-circuiting the windings at low voltage. The total losses P_t can be calculated using the following relationship [61]–[64]:

$$P_t = P_{nl} + P_{ll} = P_{jt} + P_{ec} + P_{ocl} \quad (8)$$

where, P_{nl} express the no-load losses; P_{ll} represent the load losses, P_{jt} represents the total electric losses in the windings; P_{ec} are the eddy current losses in the windings; P_{ocl} represent the other stray lossesin the transformer components.

The total additional losses is corresponded to the sum of the eddy current losses in the windings and the other stray losses in the transformer components, are calculated as follows [61]–[64].

$$P_{tol} = P_{ii} - P_{jt} = P_{ec} + P_{ocl} \quad (9)$$

The Joule losses due to the fundamental and harmonic currents are given by the following formula in the case of a resistive load [61]–[64]:

$$P_{jt} = R_t \sum_{h=1}^{h=n} I_h^2 \quad (10)$$

where, R_t is the winding resistanceof transformer; I_h is the current at the harmonic rank h.

In the presence of harmonics, eddy current losses vary with the square of the current and the square of the harmonic order. These losses can be written as follows [61]–[64]:

$$P_{ec} = P_{ec-r} \sum_{h=1}^{h=n} \left(\frac{I_h}{I_R}\right)^2 h^2 \quad (11)$$

where, P_{ec-r} are the eddy current losses in the windings under nominal conditions.

Other stray losses in a transformer are also affected by the presence of current harmonics and are generally proportional to the square of the current, with a harmonic PF not exceeding 0.8. They are written as follows [61]–[64]:

$$P_{osl} = P_{osl-r} \sum_{h=1}^{h=n} \left(\frac{I_h}{I_R}\right)^2 h^{0.8} \quad (12)$$

where, P_{ocl-r} are the other stray losses in the conductive elements under nominal conditions

In order to be able to calculate the eddy current losses in the windings and the eddy current losses in the conductive elements other than the windings, it is necessary to know these losses at 50 Hz. According to IEEE C57.110, the nominal value of additional losses represents 67% of the total additional losses for oil-immersed transformers and 33% for dry-type transformers. This American standard proposed specific coefficients following laboratory work that allow for the estimation of both types of losses in the presence of harmonics [61]–[64]. The K_f factor determines the class of transformers capable of handling non-sinusoidal loads without overheating. This factor is estimated by harmonic analysis of the load current and can be calculated using the following relationship [61]–[64].

$$K_f = \sum_{h=1}^{h=n} \left(\frac{I_h}{I_R}\right)^2 h^2 \quad (13)$$

The harmonic loss coefficient F_{hl} is represented as the ratio between the eddy current losses in the transformer windings due to harmonics and these losses under normal operating conditions; it is expressed by the following relation [61]–[64]:

$$F_{hl} = \frac{P_{ec-h}}{P_{ec-r}} = \sum_{h=1}^{h=n} \left(\frac{I_h}{I_R}\right)^2 h^2 \quad (14)$$

where, P_{ec-h} represents the eddy current losses due to harmonics.

Similarly, the factor F_{hl-ocl} for additional losses can be determined as follows [61]–[64]:

$$F_{hl-ocl} = \frac{P_{ocl-h}}{P_{ocl-r}} = \sum_{h=1}^{h=n} \left(\frac{I_h}{I_R}\right)^2 h^{0.8} \quad (15)$$

where, P_{ocl-h} represents the additional losses under harmonics.

2.2. Harmonic filtering techniques

A harmonic filter is a device that reduces harmonics in electrical installations to acceptable levels, as detailed in IEEE Standard 519. This standard is one of the most widely used standards, as it recommends all practices and requirements for controlling harmonics that distort voltage and current in electrical power and specifies their permissible limits at the common coupling point (CCP). To minimize harmonics in electrical network equipment, the most common and widely used filtering devices are divided into three categories: passive filter, active filter, and hybrid filter [11]–[18].

The damped passive filter is frequently used because of its low impedance over a wide frequency band, allowing it to simultaneously attenuate multiple harmonics. This filter offers better quality and greater reliability; it is considered a more economical and relevant choice when filtering a wide range of harmonics is required [35]. However, the filter’s resistance results in a power loss during operation at the fundamental frequency. Thanks to its unique filtering properties, this filter can address problems related to higher-order harmonics [65]–[67]. The typical design of a passive filter aims to satisfy the reactive power required by the harmonic source at the fundamental frequency, which determines the sizing of the electrical reactance's of the passive filter intended for installation on the main bus of the industrial system. The values of these reactances are calculated using the following equations [68]–[70].

$$X_{Cf} = \frac{V_1^2}{Q_c} \tag{16}$$

To trap the harmonic rank h_n, the inductive reactance of the filter must be equal to:

$$X_{Lf} = \frac{X_{Cf}}{h_n^2} \tag{17}$$

the resistance of the filter is deduced from the quality factor Q_F of the filter by the relation [35], [68]–[70]:

$$R_f = \sqrt{X_{Lf} \times X_{Cf}}/Q_F \tag{18}$$

the quality factor Q_F is a quantity that determines the bandwidth of the filter; it presents a measure of the sharpness of the tuning frequency.

The reactive power required at the common connection point to change from one PF to another improved factor is calculated according to the equation mentioned previously in (7) [71]–[73].

2.3. Modelling of polluted electrical circuit

The single-line diagram of the electrical circuit under study consists of two main parts: the high-voltage source and the polluting electrical loads, which are directly connected to the common connection point (PCC). The voltage source supplies a delta - star (Δ-Y) step-down power transformer. On the low-voltage side is a nonlinear equivalent load, typically composed of three-phase asynchronous motors, office supplies such as fluorescent lamps and computers, as well as heating and air conditioning equipment. The single-phase equivalent circuit and its simplified representation are shown in Figure 1. This load is considered the source of the unwanted harmonics, which must be attenuated.

In terms of modelling, the behaviour of this electrical circuit in the presence of harmonics can be simulated by a nonlinear load with low internal impedance acting as a harmonic current generator, which is absorbed by the transformer [74]. When these harmonic currents pass through the inductive impedance of the transformer and the upstream source, they generate harmonic voltages [75], [76]; the circuit model can be simplified as illustrated in Figure 1(a). To determine the fundamental parameters of the components represented in Figure 1(b), circuit analysis theory can be applied to calculate the electrical quantities of the nonlinear load and the transformer. For the nonlinear load, the resistance represents the active component and the inductance the reactive component, which are calculated respectively as follows [74]–[76].

$$R_l = \frac{V_1^2}{P_l} \tag{19}$$

$$X_l = \frac{V_1^2}{Q_l} \tag{20}$$

Where, P_l represents the active power dissipated by the nonlinear load; Q_l defines the reactive power consumed by the nonlinear load.

Harmonics are injected into the transformer due to the nonlinear load connected to its secondary winding, thus reducing its overall efficiency. Consequently, the calculation of the main components of a power transformer is based on its nominal parameters. The two-winding impedance is calculated from the short-circuit voltage expressed as a percentage, while the resistance and reactance are calculated from the transformer characteristics [74]–[76]. The equivalent transformer impedance is calculated using (21).

$$Z_{tr} = \sqrt{R_{tr}^2 + (\omega L_{tr})^2} = \left(\frac{Z_{sc}}{100}\right)\frac{U_{2t}^2}{S_t} \tag{21}$$

Where, U_{2t} is the secondary phase-to-phase voltage of the transformer; S_t is the transformer's apparent power; Z_{sc} is the short-circuit impedance of the transformer expressed as a percentage:

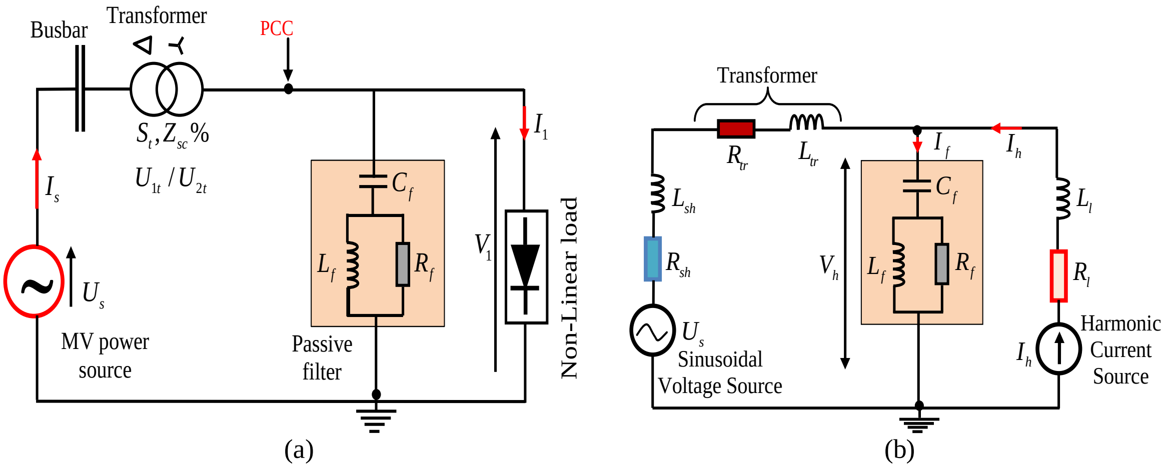

Figure 1. Single-phase equivalent circuit diagram of electrical system; (a) modelling of electrical circuit components and (b) simplified single-phase representation

Power transformer ratio X_{tr}/R_{tr} is required to determine the fundamental resistance and reactance values of the transformer. In power distribution, reactance is generally much higher than resistance [74]–[76].

The upstream supply impedance is calculated in the same way as before, from the typical values given, in particular the short-circuit impedance and the reactance/resistance ratio X_{sh}/R_{sh} it is given by the formula below [74]–[76]:

$$Z_{sh} = \sqrt{R_{sh}^2 + (\omega L_{sh})^2} = \left(\frac{Z_{sc}}{100}\right)\frac{U_S^2}{S_S} \tag{22}$$

Indeed, the harmonic voltages across the considered load, on the low-voltage side of the transformer, and across the power supply are generally calculated using the following relationship [74]–[76]:

$$V_h = I_h(Z_{sr} + Z_{tr}) \tag{23}$$

To measure the effect of harmonics on equipment connected to the electrical network through the THD of voltage and current, according to IEEE Standard 519-2014, it was necessary to determine the different ranges of voltage applied to the busbar and the short-circuit ratio at the point of common coupling (PCC). Generally, with a THD voltage below 5%, there is no problem. Between 5 and 7%, sensitive devices risk malfunctioning. Between 7 and 9%, it is the so-called normal devices that can malfunction. Finally, beyond 9%, almost all equipment risks malfunctioning or even being destroyed in the short, medium or long term [35], [70]–[75]. According to IEEE Standard 519-2014, if the voltage applied to the busbar is between 1 kV and 69 kV, the maximum permissible THD voltage is 5%. Regarding the permissible limit of the THD of the current, the short circuit ratio can be calculated using the following relationship [35], [71]–[76]:

$$SCR = \frac{I_{sc}}{I_{max}} \tag{24}$$

where, I_{sh} is the maximum short circuit current at PCC; I_{max} is the maximum demand load current at PCC.

The values of these currents can be identified respectively as follows [35], [71]–[76]:

$$I_{sc} = \frac{1000 S_{sc}}{\sqrt{3}U_{2t}} \tag{25}$$

$$I \frac{S_t}{\sqrt{3}U_{2t}}_{max} \tag{26}$$

where, S_{sc} is the short-circuit apparent power; S_t is the transformer rating power.

The three phase short circuit capacity and the line voltage are expressed in megavolt-amperes (MVA) and kilovolts (kV), respectively.

From a calculation perspective, the total demand distortion (TDD) criterion can be added as an important indicator used to assess the quality of electrical power, particularly with regard to the effect of harmonics according to IEEE 519 standards. It is determined by the following relationship [77]:

$$TDD = \frac{\sqrt{\sum_{h=2}^{h=n} I_h^2}}{I_{max}} \quad (27)$$

2.4. Application of an optimization algorithm

In this subsection, the TLBO optimization algorithm is used to determine the optimal parameters of the passive harmonic filter from an objective function subject to technical constraints. An economic analysis is also performed to evaluate the overall cost of the resulting solution.

2.4.1. Teaching learning-based optimization (TLBO)

TLBO is a new global meta-heuristic optimization method originally developed by Rao et al in 2014. It is an algorithm inspired by the teaching-learning process and is based on the effect of a teacher's influence on the output of students in a class [46]. The algorithm describes two basic modes of learning: through the teacher, known as the teacher phase, and through interaction with other students, known as the learner phase. First, the boundary ranges of all decision variables subject to optimization are defined based on technical justifications related to the characteristics of the considered system and its operating requirements. Thus, an initial set of solutions is randomly generated within the search space bounded by the minimum and maximum values of each decision variable. This initialization process is performed using the following equation [75]–[79].

$$X_{i,j} = Xij, min_{j,max}{}_{j,min} \quad (28)$$

Where, r_i is a random number from the uniform distribution, it belongs to the interval [0, 1]; $X_{j,max}$ and $X_{j,min}$ are the minimum and maximum values of the design variables.

In the teacher phase, within the class, each learner X_i learns from the best learner $X_{T,i}$ identified in the population, the difference between the teacher's result for each subject and the existing average result for each subject is given by [75]–[79]:

$$Diff_i = r_i(X_{T,i} - T_F \times M_i) \quad (29)$$

where, M_i is the average of all students in the class; T_F is the teaching factor, which is equal to 1 or 2, it serves to underline the importance of the average quality of learners h^{mean}.

Through the mechanisms of teaching and knowledge transfer to learners, the difference is updated in the teacher's phase according to the following relationship [75]–[79]:

$$X'_{k,i} = X_{k,i} + Diff_i \quad (30)$$

where, $X'_{k,i}$ defines the updated value of $X_{k,i}$. If $X'_{k,i}$ is a more distinctive solution than $X_{k,i}$ then it succeeds it, otherwise it will be ignored.

In the learning phase, the learning process by social interaction between two students, A and B, at each exam (i) for minimization is given as follows [75]–[79]:

$$X''_{A,i} = \begin{cases} X'_{A,i} + r_i(X'_{A,i} - X'_{B,i}) if(X'_{A,i} \succ X'_{B,i}) \\ X'_{A,i} + r_i(X'_{B,i} - X'_{A,i}) if(X'_{B,i} \succ X'_{A,i}) \end{cases} \quad (31)$$

where, $X'_{A,i}$ and $X'_{B,i}$ are the updated function values; $X''_{A,i}$ is accepted if it obtains the best function value.

A learner population size of 20 is adopted, with a maximum of 100 iterations. The iterative process continues until the algorithm's stopping criterion is met by reaching the predetermined maximum number of iterations.

It is important to emphasize that the basic Teaching–Learning Based Optimization (TLBO) algorithm updates solutions through both the teaching and learning phases without requiring algorithm-specific control parameters. Unlike many other population-based metaheuristic algorithms, which rely on several tuning parameters that strongly influence convergence behavior and may lead to premature convergence or suboptimal solutions, TLBO operates in a parameter-free manner. Only common settings such as population size and maximum number of iterations are required. This eliminates parameter tuning effort, reduces user bias, and simplifies implementation. Consequently, TLBO offers lower algorithmic complexity, robust convergence behavior, and efficient performance for continuous and nonlinear optimization problems, making it particularly suitable for engineering applications requiring computational efficiency and deterministic behavior under practical constraints [80]–[83]. The pseudo-code of the basic TLBO algorithm is described in Table 1 [83]–[85].

Table 1. Pseudo-Code of the TLBO algorithm

Pseudo-Code of the TLBO algorithm
1: Initialize the algorithm parameters, population size, number of decision variables, maximum number of iterations and objective function.
2: Randomly generate an initial population by assigning random values to variables representing ratings ($x_{i,k}$).
3: Evaluate the objective function for populations in the exam.
4: Select the population with the best grade as a teacher and calculate $Diff_i$ for exam, according to (29), by utilizing the teaching factor T_f.
5: Calculate $X'_{k,i}$ for all populations in the exam, according to (30), compare the two solutions $X'_{k,i}$ and $X_{k,i}$,Accept the best solution for transferring to the next step.
6: Randomly select each pair of learners and update the solution according to (31) and accept the best one for the next step.
7: Evaluate the objective function for all learners, check if the stopping criterion is satisfied; otherwise, the algorithm will iterate from step (4).

2.4.2. Objective function and optimization constraints

To reduce the THDi of the current and voltage, and to compensate for reactive power by improving the PF, the objective function is to optimize the impedance elements of the passive filter. The overall PF of an electrical system is significantly affected by harmonic distortion, which necessitates its correction. Therefore, the objective function targets the dominant harmonic currents because the voltage is less affected by harmonics due to the low impedance of the transformer and the network source. The objective function adopted by the optimization algorithm for the minimization procedure aimed at selecting the parameters for better passive filter performance is given by the following formulation:

$$OF_C = \sqrt{1 - \left(\frac{cos(\varphi_1)}{\sqrt{1+(THD_i)^2}}\right)} \quad (32)$$

where; THD_i is the THD rate of current; φ_1 represents the phase angle between between fundamental voltage and current; $\cos(\varphi_1)$ is the displacement PF (fundamental).

It should be noted that this objective function formulation constitutes an integrated mathematical approach rarely used in the optimization of damped passive filters. It establishes a direct correlation between power quality and PF, defining a compromise between the THD, the displacement factor, and the overall PF.

This demonstrates that the objective function evaluates not only the fundamental phase shift but also the harmonic degradation of the network. Thus, the optimization aims to simultaneously achieve extremely low harmonic distortion and a high- PF, guaranteeing an overall and physically consistent improvement in power quality in industrial networks. The set of variables representing the parameters of the passive filter to be optimized is as follows [86].

$$X = [R_f, L_f, C_f, Q_f, h_n] \quad (33)$$

To ensure the technical feasibility and compliance of the solutions with the sizing constraints of the passive filter, the variables are bounded by (34).

$$Xmax_{min} \quad (34)$$

The optimization problem constraints are defined according to IEEE 519 standard and CCP power quality requirements and must be checked during the optimization process to ensure effective reduction of current and voltage harmonics and PF improvement, as shown in (35).

$$THD_v \leq THD_{v(max)}$$

$$THD_i \leq THD_{iv(max)}$$
$$TDD \leq TDD_{(max)}$$
$$0.95 \leq cos(\varphi_1) \leq 1 \quad (35)$$

In accordance with IEEE 519, optimization constraints require that THDv, THDi, and TDD remain below the permissible limits of the PCC. The TDD is determined based on the SCR ratio and is considered the main indicator of compliance with harmonic current standards.

2.4.3. Economic analysis of the passive harmonic filter

The economic feasibility study of the proposed passive harmonic filter is a crucial step in assessing its practical viability in industrial electrical systems. Beyond improving power quality and reducing harmonic distortion, the filter design must be economically viable. To this end, the total cost of the filter can be estimated from the cost of its main passive components, namely capacitors, inductors, and resistors. This assessment determines the compatibility of the achieved technical performance with the implementation cost, thus providing an essential criterion for deciding whether to adopt the proposed filter in practical applications [87]–[92]. The total cost of a passive harmonic filter can be calculated based on its basic components using the technical and economic function described below [93]:

$$C_F = C_C + C_L + C_R + C_E \quad (36)$$

where; C_C is the capacitor cost; C_L is the inductor cost, C_R iS the resistor cost and C_E represents the cost associated with the energy losses during the filter lifetime.

This relationship can be written in the following form [93], [94].

$$C_F = (K_C \times Q_C) + (K_L \times Q_L) + (K_R \times P_R) + C_E \quad (37)$$

Where; K_C is the unit cost of the capacitor expressed in Algerian Dinars (AD/Mvar); Q_C represents the total capacitive reactive power as a function of the size of the passive filter in (Mvar); K_L is the unit cost of the inductor expressed in (AD/Mvar); Q_L constitutes the overall inductive reactive power as a function of the size of the passive filter in (Mvar); K_R is the unit energy cost of losses in the resistor (AD/MW); P_R is the active losses in the resistance of the passive filter in (MW).

On the other hand, the cost of energy losses can be determined in the national currency using the following relationship [93]:

$$C_E = K_{Ec}\left(\frac{h^2}{h^2-1}\right)\left[S_h + \frac{V_1^2 I_h^2}{h^2 S_h}\right] \quad (38)$$

where; S_h is the reactive power of the filter arm at harmonic order h (Mvar); V_1 is the fundamental phase-to-neutral voltage (kV); I_h represents the harmonic current of order h (A); h corresponds to the harmonic order.

It should be noted that the parameter K_{Ec} represents a discounted economic factor calculated from the following data: N_{day} represents the number of days in a year; N_{hour} expresses the number of hours in one day; the cost of energy losses C_e (AD/kWh); n_l is the lifespan of the passive filter in (years); the interest rate i_r which is expressed as a percentage (%); the utilization factor U_f and the specific losses of the capacitor P_s (kW/MVA) [93].

$$K_{Ec} = P_s \times N_{hour}N_{day} \times U_f \times C_e \times \left(\frac{(1+i_r)^{n_l}-1}{i_r(1+i_r)^{n_l}}\right) \quad (39)$$

The parameter values and average cost in national currency shown in the Table 2 can be used to calculate the total cost before and after the optimization process. To analyse the effect of harmonic current distortion, harmonic distortion measurements were performed using a Fluke 438-II power analyser directly connected to the low-voltage output of a distribution transformer, as described in Figure 2. The study focuses primarily on the first phase, assuming a balanced three-phase distribution. The harmonic spectrum diagram in Figure 3 shows the harmonic current distribution up to the seventeenth harmonic of an IMEFY 1250 kVA, 30/0.4 kVA power transformer, measured on November 11, 2025, at 10:28 AM. In addition, a Socomec multifunction measuring device (DIRIS A20) is used to monitor current, voltage, active, reactive and apparent powers, frequency and PF for LV network. The electrical measurement data from DIRIS A-20 multifunction meters, for the electrical quantities of equivalent nonlinear load, are presented in Table 3.

Table 2. Values of the coefficients and average unit costs according to the Algerian tariff

Parameter	Average value
K_C (AD/Mvar)	15000
K_L (AD/Mvar)	80000
K_R (AD/kW)	2200
P_s (kW/Mvar)	0,4
N_{hour} (Hours)	24
N_{day} (Days)	365
C_e (AD/kWh)	5.5
i_r (%)	5
n_l (Years)	15
U_f	1

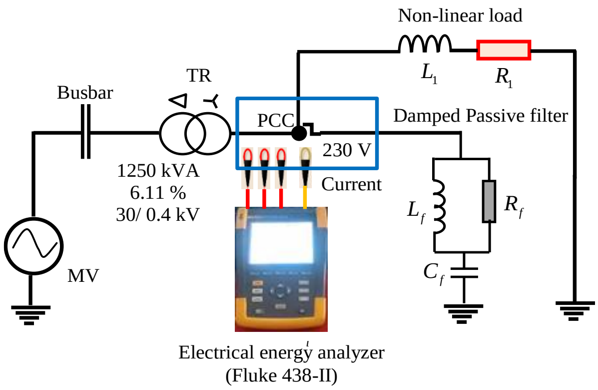

Figure 2. Schematic representation of industrial installation studied with the implementation of passive filter

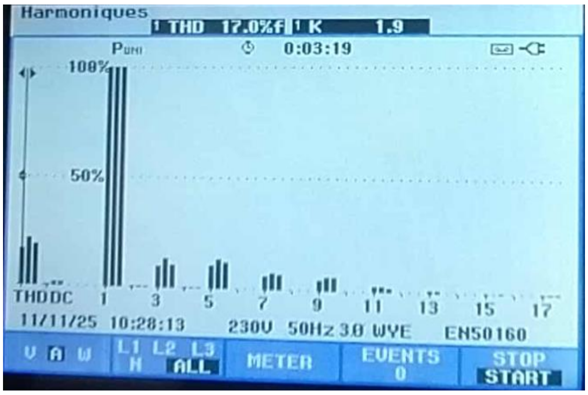

Figure 3. Spectrogram of harmonic currents created by nonlinear load

Table 3. Values of measured electrical quantities for non-linear load

Electrical quantities	Measured values
Rated voltage	230 V
Active power consumption	41.53 kW
Absorbed current	171.2 A
PF	0.78
Current frequency	50 Hz

3. RESULTS AND DISCUSSION

The first step consists of determining the THD of the current (due to loads) and voltage (at the source), and then sizing the damped passive filter in a conventional manner, by calculating its impedance components based on the capacitive reactive power required to improve the PF to the target value of 0.96, and thus evaluating the effectiveness of the passive filter in attenuating harmonic disturbances.

To analyze the impact of harmonics on the electrical network, Figure 4 represents the evolution of the THD rate in current and voltage as a function of the increasing order of harmonics. These results show that the current absorbed by the load is highly polluted: with a current THD of 17.34 %, the THD in voltage reaches 8.61 %, which is generally unacceptable on the electrical grid in terms of current, as it may lead to electrical devices being at risk of malfunction.

As shown in Figure 5, increasing the PF from 0.78 to 0.96 involves the introduction of capacitive energy, provided that it balances the active power. This figure indicates that the relationship between reactive power compensation and PF correction is approximately linear. The reactive power supplied by the compensation capacitor was 21.21 kVAR, so the new value becomes 12.11 kVAR instead of 33.32 kVAR, and the PF has been increased to improve the efficiency and stability of the electrical network and reduce energy losses.

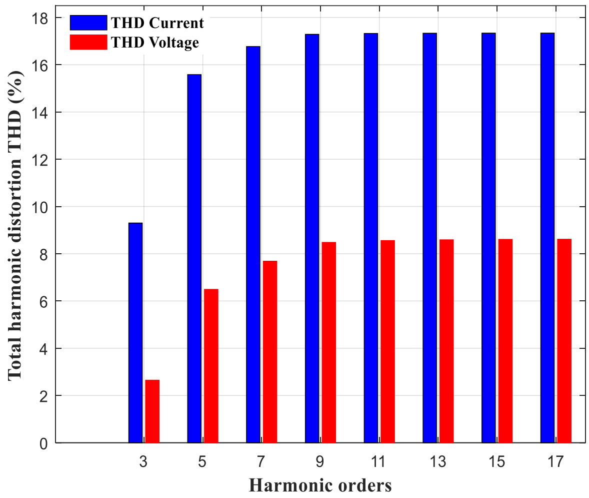

Figure 4. Determination of THD rate of current and voltage

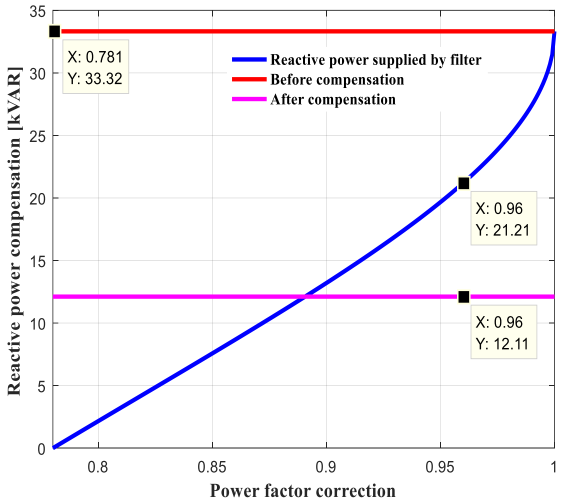

Figure 5. PF improvement by reactive power compensation

Figure 6 illustrates the passive filter sizing procedure for determining the values of the basic electrical components of the RLC as a function of the harmonic order to be eliminated and the reactive power required for compensation, using several quality factor values. Based on the current harmonic distortion rate indicated earlier, the 5th harmonic is the dominant harmonic of the nonlinear load. The passive filter is therefore tuned to a harmonic order close to the dominant harmonic to be eliminated. Consequently, the passive filter is designed according to the typical values shown in this figure, with a quality factor of 5, which is commonly used because it offers a good compromise between filtering efficiency and resonance damping.

Figure 7 tracks the harmonic spectrum of the source current before and after filtering. It can be seen that the harmonic spectrum value decreased significantly after the passive filtering process in all harmonic orders, particularly in the order in which the filter was tuned.

A traditionally sized damped passive filter can significantly improve power quality. Current THDi decreases from 17.34% to 6.67%, a reduction rate of 61.53%, while voltage total harmonic distortion (THDv) decreases from 8.61% to 3.18% (a reduction rate of 63.02%). Similarly, total demand harmonic distortion (TDD) is reduced from 2.05% to 0.80% (a reduction rate of 61.21. According to IEEE 519, the short-circuit ratio (SCR) is estimated at 19.4, and the maximum permissible TDD at the CCP is 5%. The TDD value obtained, 0.64%, is therefore well below this limit. Furthermore, the post-filtering THDi value of 6.67%, compared to 17.34% before compensation, confirms a substantial reduction in harmonic currents. Similarly, the THDv value of 3.18% meets the recommended threshold of 5%. While THDi is an excellent indicator for monitoring the distortion specific to individual equipment at a given moment, TDD is the only standard measurement required by IEEE 519 to verify the overall compliance of an installation. In general, these results demonstrate the relative effectiveness of the passive filter in reducing harmonic pollution and improving overall power quality, while meeting the requirements of IEEE 519.

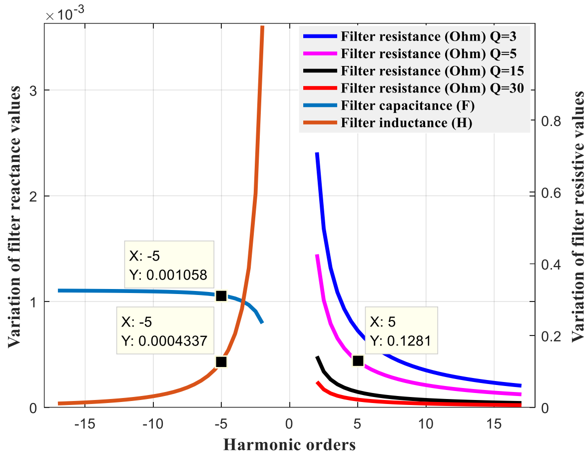

Figure 6. Typical design of passive filter elements in terms of harmonics number

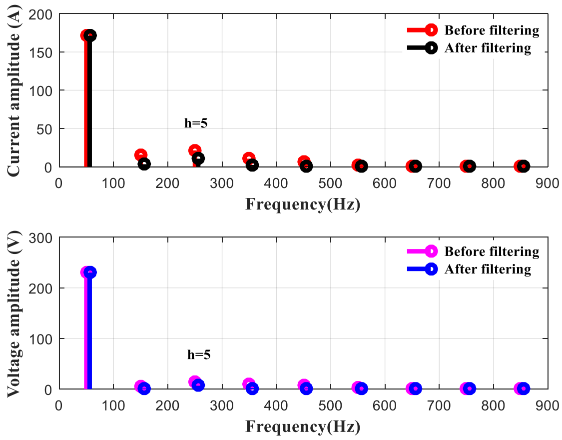

Figure 7. Harmonic spectrum of the current resulting from the network

Figures 8 and 9 depict the ability of the damped passive filter to reduce THD in current and voltage to prevent faults and improve energy efficiency. A significant reduction in THD in both current and voltage is observed, reaching extremely low amplitudes after filtering, without affecting the proper functioning of the electric grid. This demonstrates the relative performance of the filter designed to reduce overall harmonic distortion.

Figure 10 demonstrates the time evolution of the harmonic current trapped by a second-order damped passive filter, connected to the harmonic rank to be filtered (fifth order) and in parallel with the polluted load. The variation in the amplitude of the total trapped harmonic current, between reduction and increase, is due to the damping of the passive filter, which acts to adequately reduce the harmonic distortion of the electrical installation by absorbing it and diverting it to ground, thus preventing its propagation to the rest of the electrical network.

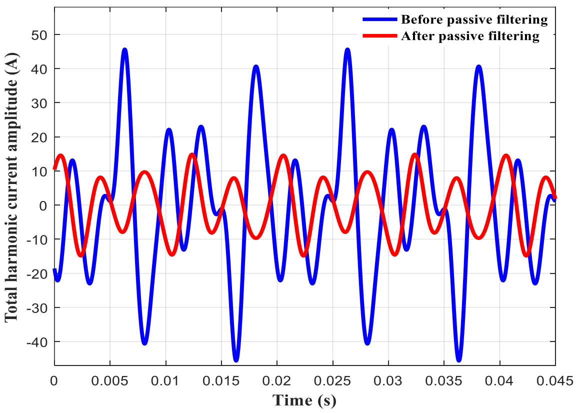

Figure 8. Harmonic current curves before and after passive filtering

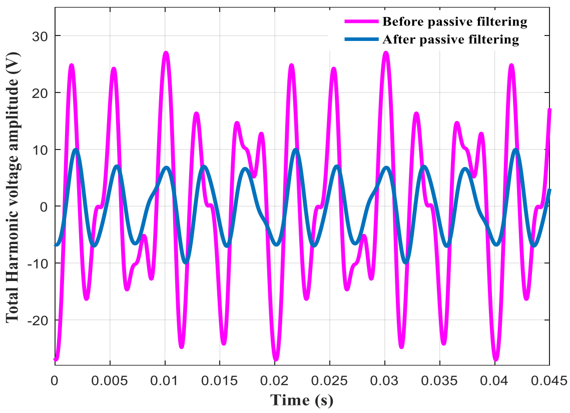

Figure 9. Harmonic voltage curves before and after passive filtering

The second step involves determining the optimal values for the elements that govern the performance of the passive filter. Therefore, a fair comparison was conducted of the performance of some of the most commonly used optimization techniques to obtain the best possible result for the estimated target values of the various parameters that affect the THD of the current. To solve the constrained optimization problem, the search areas for the variables to be optimized were defined using the objective function minimization process described in (32). These algorithms were programmed in the MATLAB (R2016b) environment on a Windows 11 operating system with an Intel(R) Core(TM) i5-1335U processor at 1.3 GHz and 16 GB of RAM.

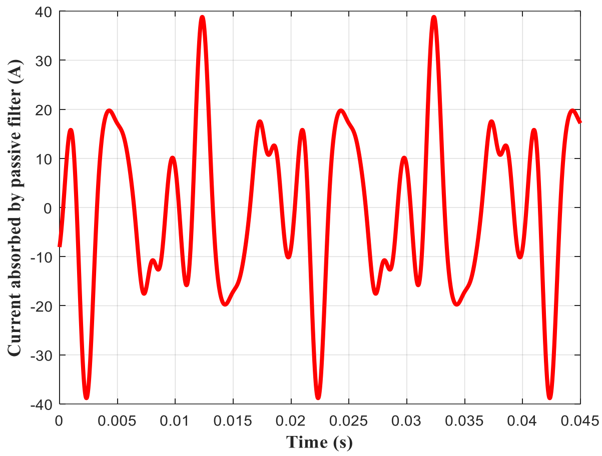

Figure 10. Fifth-order harmonic current trapped by damped passive filter

To ensure a fair comparison, the experiments for each algorithm were repeated ten times, with a maximum of 100 iterations. Table 4 presents the values of the parameter settings that adjust the comparative optimization algorithms, as well as the search spaces of the passive filter variables to be optimized.

The variations in the objective function values obtained using the proposed optimization algorithms are illustrated in Figure 11. This figure illustrates the evolution of the objective function used to determine the optimal parameters of the passive filter as a function of the number of iterations of the different algorithms. The optimization process, aimed at deciding these values, relies on search regions defined for all variables, the objective of which is to minimize the THDi of the current caused by the polluting load. This figure clearly highlights that the values of the objective function decrease continuously as the number of iterations increases, and that once optimal values are obtained; they remain stable until the end of the proposed iterations. It is worth noting that the TLBO algorithm obtained the lowest target function value, indicating its accuracy and robustness compared to other algorithms.

Table 4. Parameter settings of proposed algorithms and search limits for passive filter variables

Algorithms	Parameters setting	
TLBO	N_{pop}=20	
Artificial bee colony (ABC)	N_{pop}=20; L=10; No-looker=20.	
Differential evolution (DE)	N_{pop}=20; F= 0.6; CR=0.95.	
Grasshopper optimization algorithm (GOA)	N_{pop}=20; F = 0.5; L=1.5; C_{max} = 1; C_{min} = 0.00001.	
Grey wolf optimizer (GWO)	N_{pop}=20 ,coef ϵ [0; 2],r1 and r2 ϵ [0; 1].	
PSO	N_{pop}=20,c_1=2, c_2=2, w=0.9.	
GA	N_{pop}=20,P_m=0.2, Pc=0.4.	
Limits of passive filter variable search	Resistance (Ω)	0.01 - 5
	Inductance (H)	2e-03- 1e-02
	Capacitance (F)	1e-06- 1e-02
	Target harmonic order	3-17
	Quality factor	5-30

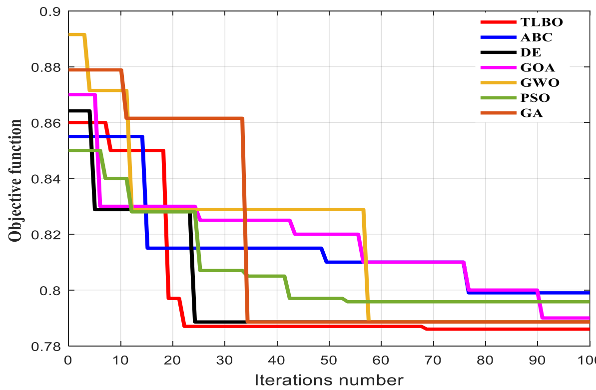

Figure 11. Variation of objective function with iterations number for different proposed algorithms

To assert the choice of this algorithm, a statistical evaluation of the results is performed using a multi-criteria decision, which included best, worst, and mean, the standard deviation of the objective function extracted from several executions, in addition to the generation and speed convergence, and the rank mean based on the Friedman test. This calculation of a certain numbers of performance indicators allows us to assess the quality of the solutions, as well as the robustness and stability of the algorithms being compared. Furthermore, the Friedman nonparametric test is applied to establish an overall ranking of the algorithms considered. Table 5 summarizes the calculation results obtained for all the algorithms considered.

Based on the performance of the different algorithms in terms of solution quality, robustness, and convergence presented in Table 5, and in order to establish a comprehensive and statistically objective comparison, the final ranking was determined using the Friedman index, where the lowest value corresponds to the best overall performance. The results show that TLBO achieves the highest Friedman index, followed by DE and PSO (3.99). Although DE exhibits the fastest convergence, TLBO provides the best performance values and maintains the highest overall ranking. In summary, the proposed TLBO algorithm achieved good results and provided more accurate data for most criteria; it can therefore be considered the most efficient and appropriate solution to the posed problem.

As a consequence, the comparison reveals that the TLBO algorithm is efficient and performs exceptionally well, making it a promising solution for optimizing the characteristic elements of the damped passive filter. The results of the impedance optimization of the passive filter components, composed of resistance (R), inductance (L), and capacitance (C), are shown in Figure 12. It appears that this algorithm converges quickly and accurately by varying all the variable values within the defined search space, until optimal values are reached after a certain number of iterations.

Furthermore, Figure 13 illustrates the result of optimizing the quality factor and target harmonic order to be trapped using the damped passive filter. After several iterations, the algorithm quickly converges to these optimal values within the defined search range. The harmonic rank value represents the maximum possible value, even if it is not the highest. This means that a high harmonic rank is extremely detrimental to power quality, even if its amplitude is small. This also avoids the filter's resonance problem with low-order harmonics.

Table 5. Statistical analysis of performance and Friedman ranking of compared optimization algorithms

Algorithms	Best	Worst	Average	Standard deviation (SD)	Iter-Conv	Conv-speed	Mean rank
TLBO	0.7860	0.86	0.7997454	0.0266626	69	0.001072464	1.65
ABC	0.799	0.855	0.81581	0.0176249909	77	0.000727273	5.05
DE	0.7886	0.864174	0.799990187	0.02162481264	25	0.003024437	2.715
GOA	0.7900	0.87	0.8180	0.0184089350	91	0.000879121	5.64
GWO	0.7886	0.891529	0.81743831	0.02964855984	58	0.001775268	4.76
PSO	0.7959	0.85	0.807866	0.01771653464	54	0.001003704	3.99
GA	0.7890	0.878854	0.8152780	0.03770744835	35	0.0025797	4.195

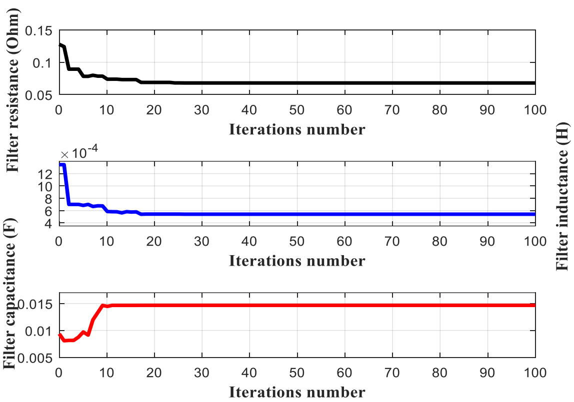

Figure 12. Convergence of optimal components of passive filter's impedance with iterations number

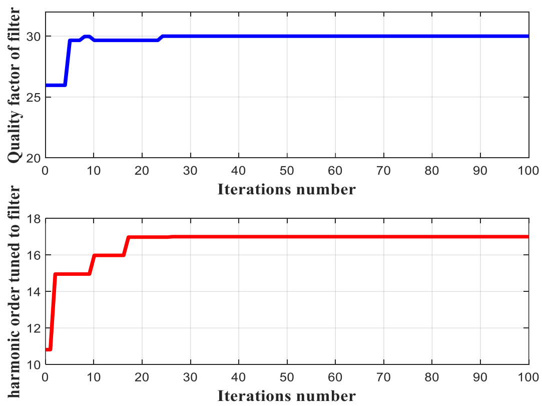

Figure 13. Convergence of optimal quality factor and tuned harmonic order values of passive filter with iterations number

Figure 14 illustrates the effect of a damped passive filter, whose parameters have been optimized by the algorithm, on the time evolution of the current Figure 14(a) and voltage Figure 14(b) applied to the nonlinear load. This effect highlights the perfect superposition of the current and voltage waveforms before and after the improved passive filtering, thus demonstrating that the final waveforms of both quantities are perfectly sinusoidal. This confirms the complete absorption of harmonics in the load current and source voltage.

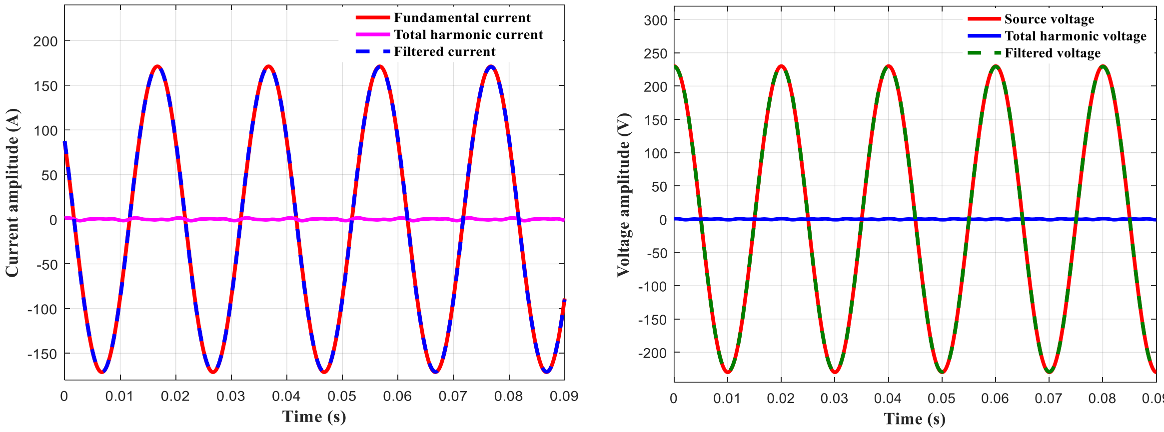

(a) (b)

Figure 14. Fundamental quantity curves without and with harmonics after optimized passive filtering (a) fundamental current curves and (b) fundamental voltage curves

Figure 15 illustrates the practical effect of the damped passive filter, showing the THD values of the current and voltage before and after the application of ordinary and optimized passive filtering. Based on the harmonic distortion analysis, the improved passive filtering ensures very low THD values for both current and voltage: 0.67% and 0.26%, respectively. These values are considered quite acceptable and do not significantly affect the proper functioning of the electrical network.

To verify the results of the harmonic distortion reduction parameters obtained through the application of the passive harmonic filter in accordance with the IEEE 519 standard, Table 6 is included, which provides a summary explicitly comparing all harmonic distortion values (before and after conventional and optimized filtering).

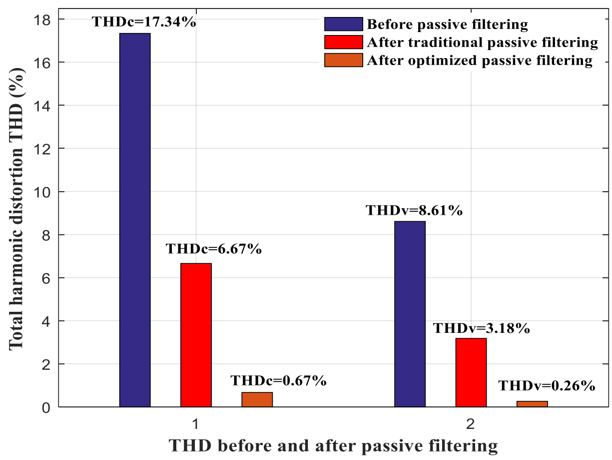

Figure 15. Determination of THD rate of current and voltage before and after optimized filtering

Table 6. Comparison of resulting THD and PF values

Parameter	IEEE-Std limit	Before filtering	After conventional filtering	After optimal filtering
THD current (%)	4	17.34	6.67	0.67
THD voltage (%)	5	8.61	3.18	0.26
TDD (%)	5	2.05	0.8	0.08
PF	/	0.78	0.96	0.978

In general, comparing costs before and after optimization enables to evaluate the compromise between the achieved filtering performance and the required investment, while also highlighting the practical aspects of implementing the optimal solution, both technically and economically. Figure 16 summarizes this comparison of total costs and shows that optimization significantly reduces the overall filter cost by approximately 49.24%. This reduction is primarily due to the decrease in capacitive reactive power requirements and the improvement in the dimensions of the main components of the passive filter. This result demonstrates the effectiveness of the proposed optimization procedure for designing a more economical filter while maintaining the required harmonic attenuation performance.

Given that the optimized passive filter is designed for specific operating conditions, its performance may be affected by variations in the industrial load. Sudden load changes can cause immediate variations in the current drawn from the electrical grid, thereby influencing the filter's harmonic mitigation capability. Figure 17 illustrates the evolution of the THDi as a function of load level. As can be observed, THDi increases progressively as the load deviates from its nominal operating condition. The passive filter achieves its best harmonic attenuation performance when operating close to the nominal load for which it was designed.

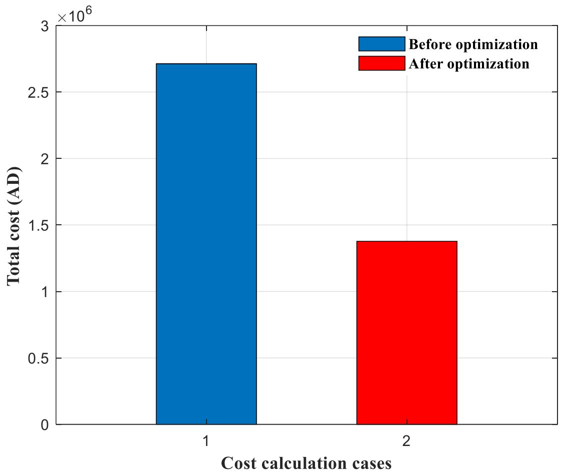

Figure 16. Comparing the average total cost of a passive filter before and after the optimization process

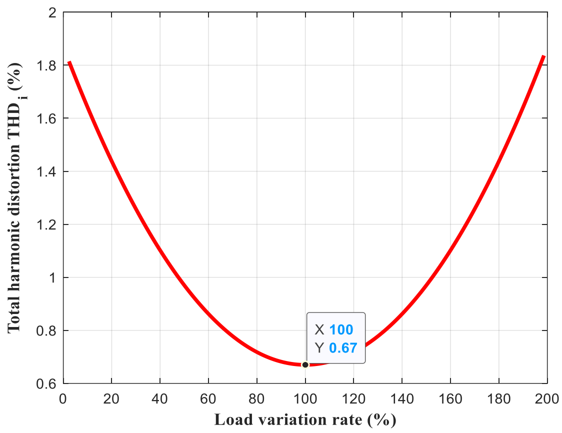

Figure 17. Sensitivity of passive filter to dynamic variation in industrial load

To quantify losses due to harmonic currents, it can be based mainly on the electrical parameters of the transformer. These include the equivalent resistance of the primary and secondary windings, the secondary current, hysterical losses and eddy current losses, as well as the nominal copper losses and the parameters initially developed to evaluate the effect of harmonic heating of the current in transformers.

Figure 18 illustrates the evolution of total losses in the distribution transformer as a function of the current absorbed by the nonlinear load before and after filtering. Initially, the losses increase gradually and slowly with increasing harmonic currents emitted by the pollutant load. As the number of harmonics in the current spectrum increases, and the THDi in current increases, the losses increase sharply, particularly with increasing current through the nonlinear load. It should be noted that the THD value of the current, which amounts to 17.34%, leads to a significant increase in losses resulting from the displacement of harmonic currents.

The difference between the total harmonic loss and the calculated loss from the fundamental harmonic reflects the effect of the non-sinusoidal currents flowing in the transformer windings on the total loss, as there is a proportional relationship between the total loss and the ratio of the THD of the current, in addition to an important factor which is the load rate according to the condition in which the harmonic measurements were taken. After ordinary filtering, the loss decreases significantly as the number of harmonics in the current spectrum increases and the total THDi in current decreases, after optimized filtering, the loss decreases even further. That is, it can be concluded that the increase in loss is directly related to the increase in the amount of absorbed current. It is important to note that a significant increase in loss, especially under heavy load rates, can reduce the transformer's lifespan and significantly impact the efficiency of the electrical grid.

As shown in Figure 19, the improved capacitor capacitance value of the passive filter allows increasing the PF from 0.78 to 0.978 and compensating reactive power with a value of 24.46 kVAR. The adopted TLBO algorithm has proven its high efficiency and reliability in selecting the optimal design values for the passive filter, in terms of robust filtration and good compensation of reactive power.

Finally, the results clearly confirm that the TLBO optimization strategy adopted is the most effective in achieving a relatively optimal solution, as it allows for the almost complete elimination of harmonic distortion in the electrical network, which has a positive impact on maintaining equipment lifespan, improving power quality and increasing efficiency.

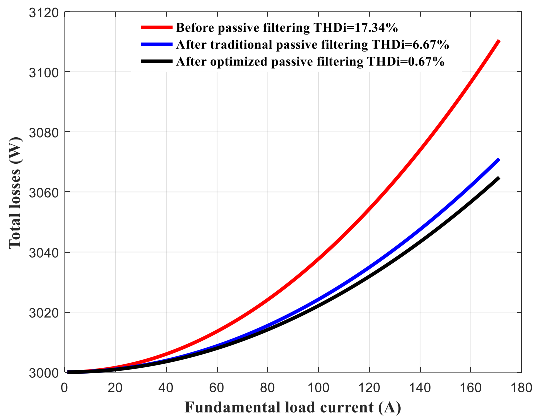

Figure 18. Total losses as a function of fundamental load current before and after optimized filtering

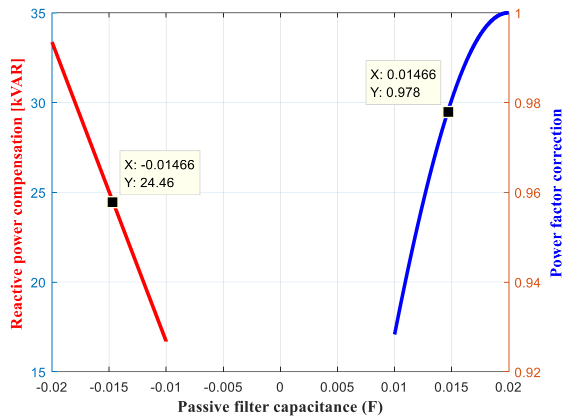

Figure 19. Effect of optimized capacitance of passive filter on PF correction and reactive power compensation

4. CONCLUSION

The phenomenon of harmonic pollution in electrical grid is becoming a major concern with the increasing use of non-linear loads. It distorts the source current shape and generates dangerous harmonic voltage, increasing energy losses and degrading electrical power quality. To overcome the harmonic pollution problem, it is essential to apply well-adapted solutions using passive, active, or even hybrid filters. In this paper, a damped passive filter is used to suppress harmonics through a design based on analytical calculations and optimal sizing based on the TLBO meta-heuristic optimization algorithm. According to the simulation results, before applying the filter, the THD of the current was approximately 17.34%, and for the voltage, it was 8.61%. After applying the ordinary filter, the THD of the current decreased to 6.67%. Similarly, the THD value for the voltage was reduced to 3.18%. The results also showed that the passive filter designed using the TLBO algorithm absorbed all the harmonics considered, and the THD of the current and voltage has decreased considerably, to the point of now reaching values that can be considered negligible. The effect of harmonics in transformers primarily leads to increased energy loss, resulting in a rise in operating temperature and consequently, overheating. Since equipment lifespan is directly related to operating temperature, the presence of harmonics will ultimately reduce the actual service life of the transformer. Therefore, monitoring the THD of the current is recommended in electrical grids using transformers. Finally, it can be concluded that the use of TLBO algorithm improved the filtering performance and compensation characteristics of the passive filter and significantly reduced the overall harmonic distortion ratio of current and voltage, as well as the costs of the passive filtering components and the energy loss cost. This highlights the robustness and reliability of the proposed algorithm.

ACKNOWLEDGEMENTS

The authors would like to thank the head the and staff of Laboratory for Analysis and Control of Energy Systems and Electric Systems, LACoSERE, University of Amar Telidji, Laghouat (03000), Algeria.

REFERENCES

[1] S. Khalid and B. Dwivedi, “Power quality issues, problems, standards and their effects in industry with corrective means,” *International Journal of Advances in Engineering and Technology (IJAET)*, vol. 1, no. 2, pp. 1–11, 2011.

[2] A. Kaushik and J. Varanasi, “Harmonic voltage distortions in power systems due to non linear loads,” *International Journal of Applied Power Engineering (IJAPE)*, vol. 3, no. 1, pp. 67–74, 2014, doi: http://doi.org/10.11591/ijape.v3.i1.pp67-74.

[3] M. J. Ghorbani and H. Mokhtari, “Impact of harmonics on power quality and losses in power distribution systems,” *International Journal of Electrical and Computer Engineering (IJECE)*, vol. 5, no. 1, p. 166, Feb. 2015, doi: 10.11591/ijece.v5i1.pp166-174.

[4] A. Priyadharshini, N. Devarajan, A. R. Uma Saranya, and R. Anitt, “Survey of harmonics in non linear loads,” *International Journal of Recent Technology and Engineering (IJRTE)*, no. 1, pp. 2277–3878, 2012, [Online]. Available: www.ijrte.org.

[5] H. Farooq, C. Zhou, and M. E. Farrag, “Analyzing the harmonic distortion in a distribution system caused by the non-linear residential loads,” *International Journal of Smart Grid and Clean Energy*, vol. 2, no. 1, pp. 46–51, 2013, doi: 10.12720/sgce.2.1.46-51.

[6] J. Lalotra, “Investigate the effect of different combination of loads on harmonic distortion,” *International Journal of Advanced Research in Computer Science and Software Engineering*, vol. 3, no. 8, pp. 587–590, 2013.

[7] Ł. Michalec, M. Jasiński, T. Sikorski, Z. Leonowicz, Ł. Jasiński, and V. Suresh, “Impact of harmonic currents of nonlinear loads on power quality of a low voltage network–review and case study,” *Energies*, vol. 14, no. 12, p. 3665, Jun. 2021, doi: 10.3390/en14123665.

[8] E. Osamah Saleh Al-duaij, “Harmonics effects in power system,” *Journal of Engineering Research and Applications www.ijera.com*, vol. 5, no. 2, pp. 1–19, 2015, [Online]. Available: www.ijera.com.

[9] A. Kumar, “Power quality issues and harmonics performance analysis for non-linear load in power distribution system,” in *2022 19th International Conference on Electrical Engineering, Computing Science and Automatic Control (CCE)*, IEEE, Nov. 2022, pp. 1–5. doi: 10.1109/CCE56709.2022.9975948.

[10] S. Rustemli, M. A. Satici, G. Şahin, and W. van Sark, “Investigation of harmonics analysis power system due to non-linear loads on the electrical energy quality results,” *Energy Reports*, vol. 10, pp. 4704–4732, 2023, doi: 10.1016/j.egyr.2023.11.034.

[11] IEEE-Std C57.110, “IEEE recommended practice for establishing liquid-filled and dry-type power and distribution transformer capability when supplying nonsinusoidal load currents,” Jun. 14, 2008, *IEEE, Piscataway, NJ, USA*: C57.110-2008. doi: 10.1109/IEEESTD.2018.8511103.

[12] O. Arikan, B. Kekezoğlu, and C. F. Kumru, “Effects of power quality terms on passive power filters,” *European Journal of Engineering and Technology*, vol. 4, no. 6, pp. 25–38, 2016, [Online]. Available: www.idpublications.org.

[13] A. A. Patil, R. N. Katkar, P. A. Ajit, C. P. Vijay, P. P. Patil, and S. . Patil, “Harmonic metigation using passive filter,” *International Journal of Engineering Trends and Technology*, vol. 45, no. 2, pp. 83–86, Mar. 2017, doi: 10.14445/22315381/IJETT-V45P219.

[14] Z. A. Memon, M. A. Uquaili, and M. A. Unar, “Harmonics mitigation of industrial power system using passive filters,” *Mehran University Research Journal of Engineering & Technology*, 2016, [Online]. Available: http://arxiv.org/abs/1605.06684.

[15] P. Salmeron and S. P. Litran, “Improvement of the electric power quality using series active and shunt passive filters,” *IEEE Transactions on Power Delivery*, vol. 25, no. 2, pp. 1058–1067, Apr. 2010, doi: 10.1109/TPWRD.2009.2034902.

[16] B. P. de Campos, L. A. R. de Sousa, and P. F. Ribeiro, “Mitigation of harmonic distortion with passive filters,” in *2016 17th International Conference on Harmonics and Quality of Power (ICHQP)*, IEEE, Oct. 2016, pp. 646–651. doi: 10.1109/ICHQP.2016.7783315.

[17] M. Hajjej and L. Sbita, “A new design and implementation of a three-phase four-wire shunt active power filter for mitigating harmonic problems caused by compact fluorescent lamps,” *Engineering, Technology and Applied Science Research*, vol. 14, no. 3, pp. 14619–14627, 2024, doi: 10.48084/etasr.7251.

[18] P. Z. Fang, “Harmonic sources and filtering approaches,” *IEEE Industry Applications Magazine*, vol. 7, no. 4, pp. 18–25, 2001.

[19] J. Afonso, C. Couto, and J. Martins, “Active filters with control based on the p-q theory,” *IEEE Industrial Electronics Society*, vol. 47, pp. 5–10, 2000, [Online]. Available: http://hdl.handle.net/1822/1921.

[20] H. H. Kuo, S. N. Yeh, and J. C. Hwang, “Novel analytical model for design and implementation of three-phase active power filter controller,” *IEE Proceedings: Electric Power Applications*, vol. 148, no. 4, pp. 369–383, 2001, doi: 10.1049/ip-epa:20010433.

[21] Y. Hoon, M. Mohd Radzi, M. Hassan, and N. Mailah, “Control algorithms of shunt active power filter for harmonics mitigation: a review,” *Energies*, vol. 10, no. 12, p. 2038, Dec. 2017, doi: 10.3390/en10122038.

[22] D. Buła and M. Zygmanowski, “Control strategies applied to active power filters,” *Energies*, vol. 15, no. 7, 2022, doi: 10.3390/en15072408.

[23] S. Zhang, D. Li, and X. Wang, “Control techniques for active power filters,” *Proceedings - International Conference on Electrical and Control Engineering, ICECE 2010*, pp. 3493–3498, 2010, doi: 10.1109/iCECE.2010.850.

[24] V. Govindaraj and M. Priya, “Review Of Hybrid Active Power Filter Topologies And Controllers For Enhancement Of Power Quality,” *International Journal Of Pure And Applied Mathematics*, vol. 118, no. 11, pp. 29–37, 2018.

[25] S. Rechka, É. Ngandui, J. Xu, and P. Sicard, “A comparative study of harmonic detection algorithms for active filters and hybrid active filters,” *PESC Record-IEEE Annual Power Electronics Specialists Conference*, vol. 1, pp. 357–363, 2002, doi: 10.1109/PSEC.2002.1023894.

[26] S. T. Senini and P. J. Wolfs, “Systematic identification and review of hybrid active filter topologies,” *PESC Record - IEEE Annual Power Electronics Specialists Conference*, vol. 1, pp. 394–399, 2002, doi: 10.1109/psec.2002.1023900.

[27] L. Herman, K. Knez, and B. Blažič, “Design and performance evaluation of a hybrid active power filter controller,” *Energies*, vol. 17, no. 11, p. 2492, May 2024, doi: 10.3390/en17112492.

[28] R. Sahu, A. Jha, and V. K. Sahu, “Hybrid active power filter topologies for power quality improvement : a review,” *International Research Journal of Engineering and Technology*, vol. 06, no. 09, pp. 1279–1282, 2019.

[29] M. Aiello, A. Cataliotti, S. Favuzza, and G. Graditi, “Theoretical and experimental comparison of total harmonic distortion factors for the evaluation of harmonic and interharmonic pollution of grid-connected photovoltaic systems,” *IEEE Transactions on Power Delivery*, vol. 21, no. 3, pp. 1390–1397, 2006, doi: 10.1109/TPWRD.2005.860231.

[30] K. Daniel, L. Kütt, M. N. Iqbal, N. Shabbir, H. A. Raja, and M. U. Sardar, “A review of harmonic detection, suppression, aggregation, and estimation techniques,” *Applied Sciences*, vol. 14, no. 23, p. 10966, Nov. 2024, doi: 10.3390/app142310966.

[31] A. Arranz-Gimon, A. Zorita-Lamadrid, D. Morinigo-Sotelo, and O. Duque-Perez, “A review of total harmonic distortion factors for the measurement of harmonic and interharmonic pollution in modern power systems,” *Energies*, vol. 14, no. 20, p. 6467, Oct. 2021, doi: 10.3390/en14206467.

[32] American Bureau of Shipping, “Control of harmonics in electrical power systems,” *Control*, no. May, pp. 1–240, 2006.
[33] Transmission and Distribution Committee, “IEEE Std. 1531-2003: guide for application and specification of harmonic filters,” Jun. 12, 2003, *IEEE, Piscataway, NJ, USA*. doi: 10.1109/IEEESTD.2003.94407.
[34] IEC-Std 61000, “General guide on harmonics and interharmonics measurements for power supply systems and equipment connected thereto,” *IEC Std. 61000-4-7*, 2002, [Online]. Available: https://scholar.google.com.hk/scholar?hl=zh-CN&q=IEC+61000-4-7&btnG=&lr=#1.
[35] IEEE Std. 519-2022, “IEEE recommended practice and requirements for harmonic control in electric power systems,” *IEEE Std. 519-2022*, p. 101, 2014.
[36] EN 50160, “Voltage characteristics of electricity supplied by public electricity networks,” *European Committee for Electrotechnical Standardization-ENELEC*, 2010.
[37] Z. Juan, G. Yi-nan, and Z. Shu-ying, “Optimal design of passive power filters of an asymmetrical system based on genetic algorithm,” *Procedia Earth and Planetary Science*, vol. 1, no. 1, pp. 1440–1447, 2009, doi: 10.1016/j.proeps.2009.09.222.
[38] R. Sirjani and M. Kusaf, “Optimal design of passive harmonic filters using bee colony optimization,” in *2016 HONET-ICT*, IEEE, Oct. 2016, pp. 88–92. doi: 10.1109/HONET.2016.7753426.
[39] H. L. Ginn and L. S. Czarnecki, “An optimization based method for selection of resonant harmonic filter branch parameters,” *IEEE Transactions on Power Delivery*, vol. 21, no. 3, pp. 1445–1451, Jul. 2006, doi: 10.1109/TPWRD.2005.860261.
[40] K. Gençol, “A new optimization-based algorithm for the estimation of harmonics under power system frequency deviations,” in *31st IEEE Conference on Signal Processing and Communications Applications, SIU 2023*, IEEE, Jul. 2023, pp. 1–4. doi: 10.1109/SIU59756.2023.10223989.
[41] M. Leon, Y. Zenlander, N. Xiong, and F. Herrera, “Designing optimal harmonic filters in power systems using greedy adaptive Differential Evolution,” in *IEEE International Conference on Emerging Technologies and Factory Automation, ETFA*, IEEE, Sep. 2016, pp. 1–7. doi: 10.1109/ETFA.2016.7733571.
[42] K. Gençol, “An efficient iterative optimization-based algorithm for the real-time estimation of harmonics under power system frequency deviations,” *Engineering Science and Technology, an International Journal*, vol. 47, p. 101543, Nov. 2023, doi: 10.1016/j.jestch.2023.101543.
[43] M. L. Duc, L. Hlavaty, P. Bilik, and R. Martinek, “Harmonic mitigation using meta-heuristic optimization for shunt adaptive power filters: a review,” *Energies*, vol. 16, no. 10, p. 3998, May 2023, doi: 10.3390/en16103998.
[44] K. Chahine, “Machine learning in active power filters: advantages, limitations, and future directions,” *AI (Switzerland)*, vol. 5, no. 4, pp. 2433–2460, 2024, doi: 10.3390/ai5040119.
[45] A. Eslami, M. Negnevitsky, E. Franklin, and S. Lyden, “Review of AI applications in harmonic analysis in power systems,” *Renewable and Sustainable Energy Reviews*, vol. 154, 2022, doi: 10.1016/j.rser.2021.111897.
[46] R. V. Rao, V. J. Savsani, and D. P. Vakharia, “Teaching–learning-based optimization: a novel method for constrained mechanical design optimization problems,” *Computer-Aided Design*, vol. 43, no. 3, pp. 303–315, Mar. 2011, doi: 10.1016/j.cad.2010.12.015.
[47] H. Iqbal and A. Sarwat, “Design and implementation of hybrid GA-PSO-based harmonic mitigation technique for modified packed U-Cell inverters,” *Energies*, vol. 18, no. 1, 2025, doi: 10.3390/en18010124.
[48] N. C. Yang and S. W. Liu, “Multi-objective teaching–learning-based optimization with pareto front for optimal design of passive power filters,” *Energies*, vol. 14, no. 19, 2021, doi: 10.3390/en14196408.
[49] V. Dovgun, D. Egorov, and V. Novikov, “High-pass harmonic filters: general properties and design procedure,” in *2019 International Conference on Industrial Engineering, Applications and Manufacturing, ICIEAM 2019*, IEEE, Mar. 2019, pp. 1–4. doi: 10.1109/ICIEAM.2019.8743078.
[50] S. Saha, S. Das, and C. Nandi, “Harmonics analysis of power electronics loads,” *International Journal of Computer Applications*, vol. 92, no. 10, pp. 32–36, Apr. 2014, doi: 10.5120/16046-5228.
[51] Chih-Ju Chou, Chih-Wen Liu, June-Yown Lee, and Kune-Da Lee, “Optimal planning of large passive-harmonic-filters set at high voltage level,” *IEEE Transactions on Power Systems*, vol. 15, no. 1, pp. 433–441, 2000, doi: 10.1109/59.852156.
[52] D. M. Soomro and M. M. Almelian, “Optimal design of a single tuned passive filter to mitigate harmonics in power frequency,” *ARPN Journal of Engineering and Applied Sciences*, vol. 10, no. 19, pp. 9009–9014, 2015.
[53] S. allam and H. EI-hash, “An optimal design of single tuned filter in distribution systems,” *ERJ. Engineering Research Journal*, vol. 30, no. 1, pp. 1–8, Jan. 2007, doi: 10.21608/erjm.2007.69888.
[54] M. Usman, M. Shahzad, A. Sattar, and M. Ayaz, “Harmonics measurement in computer laboratory and design of passive harmonic filter using MATLAB,” *International Journal of Advanced Computer Science and Applications*, vol. 8, no. 12, 2017, doi: 10.14569/ijacsa.2017.081230.
[55] R. N. Beres, X. Wang, F. Blaabjerg, M. Liserre, and C. L. Bak, “Optimal design of high-order passive-damped filters for grid-connected applications,” *IEEE Transactions on Power Electronics*, vol. 31, no. 3, pp. 2083–2098, 2016, doi: 10.1109/TPEL.2015.2441299.
[56] S. S. Desai, K. H. Dattesh, and J. P. Student, “Design of shunt passive filter for reducing harmonic in variable frequency drives (VFDs): a review,” *Journal of Emerging Technologies and Innovative Research*, vol. 6, no. 5, pp. 178–183, 2019, [Online]. Available: www.jetir.org.
[57] J. C. Das, “Effects of harmonics,” in *Power System Harmonics and Passive Filter Designs*, Wiley, 2015, pp. 331–378. doi: 10.1002/9781118887059.ch8.
[58] J. Yaghoobi, A. Alduraibi, D. Martin, F. Zare, D. Eghbal, and R. Memisevic, “Impact of high-frequency harmonics (0–9 kHz) generated by grid-connected inverters on distribution transformers,” *International Journal of Electrical Power and Energy Systems*, vol. 122, 2020, doi: 10.1016/j.ijepes.2020.106177.
[59] S. Czapp, “The impact of higher-order harmonics on tripping of residual current devices,” in *2008 13th International Power Electronics and Motion Control Conference*, IEEE, Sep. 2008, pp. 2059–2065. doi: 10.1109/EPEPEMC.2008.4635569.
[60] M. Kanálik, A. Margitová, and J. Urbanský, “Calculation of power transformer losses due to harmonic current flow,” *Proceedings of the 10th International Scientific Symposium on Electrical Power Engineering, ELEKTROENERGETIKA 2019*, pp. 87–91, 2019.
[61] T. Dao and B. T. Phung, “Effects of voltage harmonic on losses and temperature rise in distribution transformers,” *IET Generation, Transmission & Distribution*, vol. 12, no. 2, pp. 347–354, Jan. 2018, doi: 10.1049/iet-gtd.2017.0498.
[62] V. León-Martínez, E. Peñalvo-López, J. A. Sáiz-Jiménez, and A. León-Vinet, “revisited concept of three-phase transformers’ short-circuit resistances in light of the institute of electric and electronics engineers (IEEE) Standard C57.110-2018,” *Applied Sciences*, vol. 14, no. 7, p. 3126, Apr. 2024, doi: 10.3390/app14073126.
[63] A. Gupta and R.Singh, “Computation of transformer losses under the effects of non-sinusoidal currents,” *Advanced Computing: An International Journal*, vol. 2, no. 6, pp. 91–104, Nov. 2011, doi: 10.5121/acij.2011.2609.

[64] O. E. Gouda, G. M. Amer, and W. A. A. Salem, “A study of k- factor power transformer characteristics by modeling simulation,” *Engineering, Technology & Applied Science Research*, vol. 1, no. 5, pp. 114–120, Oct. 2011, doi: 10.48084/etasr.59.

[65] J. Khajouei, S. Esmaeili, and S. M. Nosratabadi, “Optimal design of passive filters considering the effect of Steinmetz circuit resonance under unbalanced and non-sinusoidal conditions,” *IET Generation, Transmission & Distribution*, vol. 14, no. 12, pp. 2333–2344, Jun. 2020, doi: 10.1049/iet-gtd.2019.1755.

[66] Usman, A. Muchtar, Sujito, and W. M. Muttaqin, “Comparison between single tuned filter and c-type filter performance on the electric power distribution network,” *Journal of Physics: Conference Series*, vol. 1175, no. 1, p. 012127, Mar. 2019, doi: 10.1088/1742-6596/1175/1/012127.

[67] I. A. Shah, R. K. Ali, and N. Khan, “Design of a C-type passive filter for reducing harmonic distortion and reactive power compensation,” *International Journal of Software & Hardware Research in Engineering*, vol. 4, no. 12, pp. 38–47, 2016.

[68] M. I. Malik and E. Ihsanto, “Design and simulation high pass filter second order and c-type filter for reducing harmonics as power quality repair effort in the automotive industry,” *Journal of Integrated and Advanced Engineering (JIAE)*, vol. 3, no. 1, pp. 23–36, Mar. 2023, doi: 10.51662/jiae.v3i1.79.

[69] S. F. Moghaddam, S. Esmaeili, S. Shakeri, and M. Mohammadnejad, “Probabilistic optimal planning of passive harmonic filters in distributed networks considering possible network configurations with high penetration of non-linear loads,” *AUT Journal of Electrical Engineering*, vol. 55, no. 2, pp. 207–224, 2023, doi: 10.22060/eej.2023.21941.5499.

[70] Y. Elmi and D. Salman, “Simulation model for passive harmonic filters using Matlab/Simulink: a case study,” *Journal of Power and Energy Engineering*, vol. 11, no. 03, pp. 1–14, 2023, doi: 10.4236/jpee.2023.113001.

[71] N. M. Khattab, S. H. E. A. Aleem, T. A. Boghdady, R. A. Turky, Z. M. Ali, and M. M. Sayed, “A novel design of fourth-order harmonic passive filters for total demand distortion minimization using crow spiral-based search algorithm,” *Ain Shams Engineering Journal*, vol. 13, no. 3, p. 101632, 2022.

[72] A. Menti, T. Zacharias, and J. Milias-Argitis, “Optimal sizing and limitations of passive filters in the presence of background harmonic distortion,” *Electrical Engineering*, vol. 91, no. 2, pp. 89–100, Aug. 2009, doi: 10.1007/s00202-009-0120-3.

[73] M. Bajaj and A. K. Singh, “Optimal design of passive power filter for enhancing the harmonic-constrained hosting capacity of renewable DG systems,” *Computers and Electrical Engineering*, vol. 97, 2022, doi: 10.1016/j.compeleceng.2021.107646.

[74] R. Samikannu, R. Rohini, V. S. Kumar, and V. Mezhuyev, “Design and development of shunt active filter using MATLAB for minimization of harmonics,” *International Journal of Engineering and Technology (UAE)*, vol. 7, no. 3, pp. 179–183, 2018, doi: 10.14419/ijet.v7i3.10.15655.

[75] D. Elfando, E. M. Silalahi, S. Stepanus, B. Widodo, and R. Purba, “Reducing of total harmonic distortion using passive filter simulation to suppress harmonic currents with the case: General Hospital, Universitas Kristen Indonesia Jakarta,” *IOP Conference Series: Earth and Environmental Science*, vol. 878, no. 1, p. 012061, Oct. 2021, doi: 10.1088/1755-1315/878/1/012061.

[76] B. De-Metz-Nozblat, F. Dumas, and C. Poulain, “Calculation of short circuit currents,” *Cahier Technique Schneider Electric*, vol. 158, 2005.

[77] K. M. Alawasa and A. H. Al-Badi, “Investigation and analysis of the power quality in an academic institution’s electrical distribution system,” *Energies*, vol. 17, no. 16, p. 3998, Aug. 2024, doi: 10.3390/en17163998.

[78] D. Tang, J. Zhao, and H. Li, “An improved teaching-learning-based optimization algorithm with memetic method for global optimization,” *International Journal of Advancements in Computing Technology*, vol. 5, no. 9, pp. 942–949, May 2013, doi: 10.4156/ijact.vol5.issue9.112.

[79] H. R. E. H. Bouchekara, M. A. Abido, and M. Boucherma, “Optimal power flow using teaching-learning-based optimization technique,” *Electric Power Systems Research*, vol. 114, pp. 49–59, Sep. 2014, doi: 10.1016/j.epsr.2014.03.032.

[80] P. Sarzaeim, O. Bozorg-Haddad, and X. Chu, “Teaching-learning-based optimization (TLBO) algorithm,” in *Studies in Computational Intelligence*, 2018, pp. 51–58. doi: 10.1007/978-981-10-5221-7_6.

[81] M. M. Puralachetty, V. K. Pamula, L. M. Gondela, and V. N. B. Akula, “Teaching-learning-based optimization with two-stage initialization,” in *2016 IEEE Students’ Conference on Electrical, Electronics and Computer Science (SCEECS)*, IEEE, Mar. 2016, pp. 1–5. doi: 10.1109/SCEECS.2016.7509340.

[82] R. V. Rao and V. Patel, “An improved teaching-learning-based optimization algorithm for solving unconstrained optimization problems,” *Scientia Iranica*, vol. 20, no. 3, pp. 710–720, 2013, doi: 10.1016/j.scient.2012.12.005.

[83] O. Bozorg-Haddad, P. Sarzaeim, and H. A. Loáiciga, “Developing a novel parameter-free optimization framework for flood routing,” *Scientific Reports*, vol. 11, no. 1, p. 16183, Aug. 2021, doi: 10.1038/s41598-021-95721-0.

[84] D. Rabah, M. Lahdeb, S. Ghoneim, and D. Mahi, “Combined effects of electrostatic and electromagnetic interferences of high voltage overhead power lines on aerial metallic pipeline,” *Facta universitatis - series: Electronics and Energetics*, vol. 35, no. 3, pp. 349–377, 2022, doi: 10.2298/FUEE2203349R.

[85] S. Lu, D. Liu, D. Li, and X. Shao, “Enhanced teaching–learning-based optimization algorithm for the mobile robot path planning problem,” *Applied Sciences (Switzerland)*, vol. 13, no. 4, 2023, doi: 10.3390/app13042291.

[86] R. V. Rao and G. Waghmare, “Optimum static balancing of a robot manipulator using TLBO algorithm,” *Advances in Robotics Research*, vol. 2, no. 1, pp. 13–31, 2018, [Online]. Available: https://doi.org/10.12989/arr.2018.2.1.013.

[87] T. A. H. Alghamdi, F. Anayi, and M. Packianather, “Optimal design of passive power filters using the MRFO algorithm and a practical harmonic analysis approach including uncertainties in distribution networks,” *Energies*, vol. 15, no. 7, p. 2566, Apr. 2022, doi: 10.3390/en15072566.

[88] G. G. Richards, O. T. Tan, P. Klinkhachorn, and N. I. Santoso, “Cost-constrained power factor optimization with source harmonics using LC compensators,” *IEEE Transactions on Industrial Electronics*, vol. IE-34, no. 2, pp. 266–270, May 1987, doi: 10.1109/TIE.1987.350964.

[89] A. F. Zobaa and S. H. E. A. Aleem, “A new approach for harmonic distortion minimization in power systems supplying nonlinear loads,” *IEEE Transactions on Industrial Informatics*, vol. 10, no. 2, pp. 1401–1412, 2014, doi: 10.1109/TII.2014.2307196.

[90] H. K. M. Youssef, A. M. I. Brahim, S. H. E. A. Aleem, and E. M. M. A. Hady, “DA methodology for low-cost optimization of energy efficient passive filters in distribution networks,” *International Journal of Advanced Research in Electrical, Electronics and Instrumentation Engineering*, vol. 03, no. 12, pp. 13506–13515, Dec. 2014, doi: 10.15662/ijareeie.2014.0312048.

[91] M. Huang, W. Liu, T. Wang, H. Song, X. Li, and A. Liu, “A queuing delay utilization scheme for on-path service aggregation in services-oriented computing networks,” *IEEE Access*, vol. 7, pp. 23816–23833, 2019, doi: 10.1109/ACCESS.2019.2899402.

[92] A. F. Zobaa, “Mixed-integer distributed ant colony multi-objective optimization of single-tuned passive harmonic filter parameters,” *IEEE Access*, vol. 7, pp. 44862–44870, 2019, doi: 10.1109/ACCESS.2019.2903910.

[93] M. Kiani-Moghaddam, M. Shivaie, and P. D. Weinsier, “A techno-economic multi-objective model for hybrid harmonic filter planning considering uncertainty in non-linear loads,” *International Journal of Electrical Power & Energy Systems*, vol. 112, pp. 339–352, Nov. 2019, doi: 10.1016/j.ijepes.2019.05.013.

[94] S. M. Ismael, S. H. E. A. Aleem, A. Y. Abdelaziz, and A. F. Zobaa, “Economical design of capacitive components of multiple-arm shunt passive harmonics filters,” *Classical and Recent Aspects of Power System Optimization*, pp. 185–217, 2018, [Online]. Available: https://linkinghub.elsevier.com/retrieve/pii/B9780128124413000082.

BIOGRAPHIES OF AUTHORS

Brahimi Omar was born in Laghouat, Algeria, in 1974. He received the Engineer diploma in electrical machines from the electrical engineering department of Laghouat University in 1997-Algeria. He is Ph.D. student at the Univesity of Amar Telidji in Laghouat, Department of Electrical Engineering. Faculty of Technology, Algeria. His research interests concern: study of harmonics and power quality in electrical networks, electromagnetic compatibility, and optimization techniques. Correspondance adresse. He can be contacted at email: om.brahimi@lagh-univ.dz.

Djekidel Rabah w+as born in Laghouat, Algeria, in 1968. He graduated the University of ENSET Technique in Laghouat, Algeria, in 1991. He received the Magister and Ph.D. degrees in electrical engineering, respectively in 2010, 2015 from USTO Oran University and Laghouat University, Algeria. He is professor at the Department of Electrical Engineering, Faculty of Technology; University of Amar Telidji in Laghouat, Algeria. His research interests concern: electromagnetic interference fields, high voltage engineering, numerical modeling and simulation, and optimization Techniques. He can be contacted at email: r.djekidel@lagh-univ.dz.

Hadjadj Abdechafik was born in Laghouat, Algeria in 1976 he received the D.E.S.S degree in Monitoring and Maintenance of Electro-technical Systems in 2003 in Supervision Higher Institute of Computer Science and Automation of Lorraine, Nancy, France. In 2007 he received the Ph.D. degree in Electro-Magnetic Compatibility from University of Aix Marseille III, France. In 2008, he joined the Department of Electrical Engineering at the University of Laghouat, Algeria, as a teaching assistant. Since 2014, he has been a lecturer in the same department. He is also head of the “Diagnostic Supervision and Electromagnetic Compatibility” research team at the LACoSERE laboratory of the University of Laghouat. Since 2017, he has directed this laboratory. In 2019, he was promoted to the rank of university professor. His research focuses on the electromagnetic shielding problems of electrical equipment, the quantification and filtering of electromagnetic disturbances in power electronic systems. He can be contacted at email: a.hadjadj@lagh-univ.dz.

Bessedik Sid Ahmed was born in Frenda, Tiaret, Algeria, in 1980. He graduated the University of ibn khaldoun in Tiaret, Faculty of Technology in 2004, in Algeria. He received the magister and Ph.D. degrees in electrical engineering, respectively in 2008, 2015 from USTO Oran University, Algeria. He is professor at the University of Amar Telidji in Laghouat, Department of Electrical Engineering; Faculty of Technology-Algeria. His research interests concern: high voltage, insulation materials and dielectric, numerical modeling and simulation, optimization techniques of artificial intelligence, and fault ddiagnosis of electric machines. He can be contacted at email: s.bessedik@lagh-univ.dz.